catalysts

MDPI

Article

Synthesis and Characterization of Ca-ALG/MgO/Ag Nanocomposite Beads for Catalytic Degradation of Direct Red Dye

Hanan A. Albalwi

Department of Chemistry, College of Science and Humanities in Al-Kharj, Prince Sattam Bin Abdulaziz University, Al-kharj 11942, Saudi Arabia; h.albalwi@psau.edu.sa

Abstract: Increased water pollution due to the tremendous increase of dye-containing effluent is still a serious problem which, in turn, adversely affects aquatic life and, consequently, the balance of our ecosystem. The aim of this research was to investigate whether Ca-ALG/MgO/Ag nanocomposite beads successfully prepared from calcium alginate hydrogels with MgO (Ca-ALG/MgO) doped with Ag nanoparticles (Ag NPs) caused effective degradation of Direct Red 83 dye. The formation of nanocomposite beads was confirmed by X-ray diffraction (XRD), Transmission Electron Microscope (TEM), Dynamic Light Scattering (DLS), and Energy Dispersive X-ray Analysis (EDX). The results from the EDX analysis proved that both MgO and Ag nanoparticles within the alginate beads network were present. This study also examines the effects of various operating parameters, such as the reducing agent, time of reaction, the concentration of the dye solution, and the catalyst dosage, which were examined and studied carefully to find the optimum degradation conditions. The kinetics and isothermal study revealed that the degradation process using Ca-ALG/MgO/Ag nanocomposite beads as a catalyst in the presence of sodium borohydride ($NaBH_{4)}$ as a reducing agent was the best fit for the pseudo-first-order model and the Temkin isotherm model. The results indicated that the optimum dosage of Ca-ALG/MgO/Ag was 0.3 g for a dye concentration of 50 mg/L, and equilibrium of the degradation process was attained at 340 min. Accordingly, it could be stated that the catalyst, Ca-ALG/MgO/Ag nanocomposite beads, is considered efficient for the degradation of Direct Red 83 dye. The degradation efficiency reached 95% approximately. Furthermore, after four runs of reuse, Ca-ALG/MgO/Ag nanocomposite beads exhibited excellent performance and long-term stability.

Keywords: alginate; MgO nanoparticles; Ag nanoparticles; catalytic degradation; Ca-ALG/MgO/Ag nanocomposite

Citation: Albalwi, H.A. Synthesis and Characterization of Ca-ALG/MgO/Ag Nanocomposite Beads for Catalytic Degradation of Direct Red Dye. *Catalysts* **2023**, *13*, 78. https://doi.org/10.3390/catal13010078

Academic Editor: Francisco José Maldonado-Hódar

Received: 15 November 2022
Revised: 14 December 2022
Accepted: 22 December 2022
Published: 30 December 2022

1. Introduction

Several industries, including paper, leather tanning, plastics, cosmetics, rubber, and textile manufacturing, dump large amounts of colors into wastewater. These complex organic compounds are a significant source of pollution in the hydrosphere [1]. Organic dyes are widely utilized in various areas and cause substantial water contamination. The majority of industrial dyes are carcinogenic, poisonous, and teratogenic. A statistical data survey estimated that one million tons of such dyes are produced worldwide annually. Any artificial dye that contains the azo group (-N=N-) can be classified as an azo dye. Nucleophiles are called auxochromes, while aromatic groups are called chromophores when describing a dye molecule. The dye molecule is referred to as a chromogen when its two constituents are combined [2,3]. Because of the severe problem of dye pollution, several techniques are applied to remove toxic dyes, such as adsorption, coagulation, flocculation, membrane filtration, irradiation, concentration, and chemical transformation. These approaches, however, are costly, which limits their applicability [4]. Due to the widespread application of dye compounds and their numerous hazardous and toxic derivatives, the cleaning of wastewater by removal of color dyestuff becomes environmentally

important. In this context, the development of novel, fast, and easy techniques, such as photo-degradation of methylene blue (MB) and methyl orange (MO) azo dyes from water [5,6] for the treatment of dye-containing effluents is required.

The removal of dye from the water was studied using a variety of techniques. Physical, chemical, and biological approaches were among the methods used [7]. Adsorption, coagulation, and filtering are examples of physical approaches. Ultrasonic power, hydrodynamic cavitational techniques, sonochemical reactors, sonophotocatalytic degradation, and the photocatalyst process are all processes utilized in the degradation of dyes [8,9]. Although adsorption by low-cost materials is effective for removing dyes, it produces a lot of solid waste [10].

Brown seaweed extracts alginate is a natural polysaccharide. It has several advantages, including availability, low cost, non-toxicity, biocompatibility, and biodegradability, as well as its ability to act as an effective bioadsorbent due to carboxylate activities along its chains. Composite sorbents, such as calcium alginate beads, have recently gotten much interest since they combine the qualities and benefits of each of their constituents.

With the increased possibilities of innovative products and procedures, progress in the field of nanotechnology has created a whole new trend in wastewater treatment. Dendrimers, metal-containing nanoparticles, zeolites, and carbonaceous nanomaterials are the four types of nanomaterials that are considered particularly important materials in water treatment. Metal nanoparticles' ability to customize into numerous morphologies prompted an increase in their use in various applications [11].

Many studies have been conducted on the combination of calcium alginates with nanomaterials as metal nanoparticles [12] (Ag, Cu, Au, ...) and metal oxides (MgO, ZnO, and TiO_2) [13,14]. Ganjar Fadillah et al. (2019) modified Fe_3O_4 nanoparticles by supporting alginate as a natural polymer on the surface of Fe_3O_4 NPs and using it as a catalyst for the degradation of methylene blue dye, with the percentage of MB dye removal reaching over 90% [15]. The researchers focused on incorporating these metal nanoparticles onto the polymer support because the physicochemical properties of the polymer support, combined with the chemical properties of the polymer-bound functional groups and the catalytic efficiency of the metal nanoparticles, provide opportunities for the development of novel catalysts [11]. The catalytic degradation of dyes into smaller, safer molecules is an effective method for removing hazardous dyes [16].

The mechanism of dye degradation can occur under visible light due to the tendency of dyes to absorb some visible light. This mechanism involves dye excitation from the ground state (Dye) to the triplet excited state (Dye*) under visible light photons ($\lambda > 400$ nm). This excited state dye species is further converted into a semi-oxidized radical cation ($Dye^{+\cdot}$) by electron injection into the conduction band of the nanomaterial. Due to reactions between these trapped electrons and dissolved oxygen in the system, superoxide radical anions ($O_2^{-\cdot}$) are formed, which, in turn, result in the formation of hydroxyl radicals ($OH^{\cdot}$) [17,18]. These $OH^{\cdot}$ radicals are primarily responsible for the oxidation of the organic compounds represented by the equations below.

$$2O_2^{-\cdot} + 2H^+ \rightarrow 2HOO \rightarrow H_2O_2 \rightarrow 2OH$$

$$Dye + {}^{\bullet}OH \rightarrow CO_2 + H_2O \text{ (dye intermediates)}$$

$$Dye + h\gamma \rightarrow Dye\ *$$

$$Dye^* + catalyst \rightarrow Dye^{+} + (Catalyst)^{-}$$

In order to investigate the adsorption processes of the dye on the catalyst surface, and to quantify the photodegradation activity, kinetic study for various parameters in different conditions for the degradation process is usually considered. A previous study conducted by the author et al. [19] has reported that the degradation of basic blue 3 dye over Ca-ALG/Ag nanocomposite beads followed pseudo-second-order kinetics. Alimard [20] studied the kinetics of degradation for direct red 81 dye using Nd-Ce doped Fe_3O_4-chitosan. The kinetic study revealed that dye degradation obeyed the pseudo-second-order Blanchard

kinetic model. Amorim et al. [21] found that the degradation of direct red 83 dye by the photoperoxidation process presented nonlinear pseudo-first-order reaction kinetics. León et al. [22] investigated the effect of ultrasound on the degradation of acid brown 83 dye using seven different methods and stated that the pseudo-first-order model best describes the degradation of dye for all methods.

Variation in the sensitivity of the applied nanocomposite catalyst still serves as an attraction for researchers to study the ability of polymeric nanocomposite toward the degradation of various types of dyes.

The major goal of this research is to create ionically cross-linked nanobeads composed of Ca-ALG/MgO/Ag for dye removal by degradation in the presence of $NaBH_4$ as a reducing agent, which is capable of catalytic degradation at high concentrations of dyes. This is important as it measures the sensitivity and the ability of such catalysts with regard to degradation, even in small quantities. The prepared nanobeads were fully characterized by various techniques, and the formation of MgO and Ag NPs was confirmed and evaluated. It was observed that the degradation percentage of Direct Red 83 dye using Ca-ALG /MgO/Ag nanocomposite beads is high. The morphological behavior before and after interactions was investigated using various parameters such as catalyst amount, equilibrium time, temperature, and concentration of Direct Red 83 dye solutions at the first stage.

2. Results and Discussions

2.1. DLS and EDX of Prepared Catalyst

EDX was used for elemental identification and for determining the composition of Ca-ALG/MgO/Ag nanocomposite beads, as shown in Figure 1a. The particle size of the Ca-ALG/MgO/Ag was determined by using DLS. Results obtained from Figure 1b revealed that the average particle size was estimated to be 178 nm.

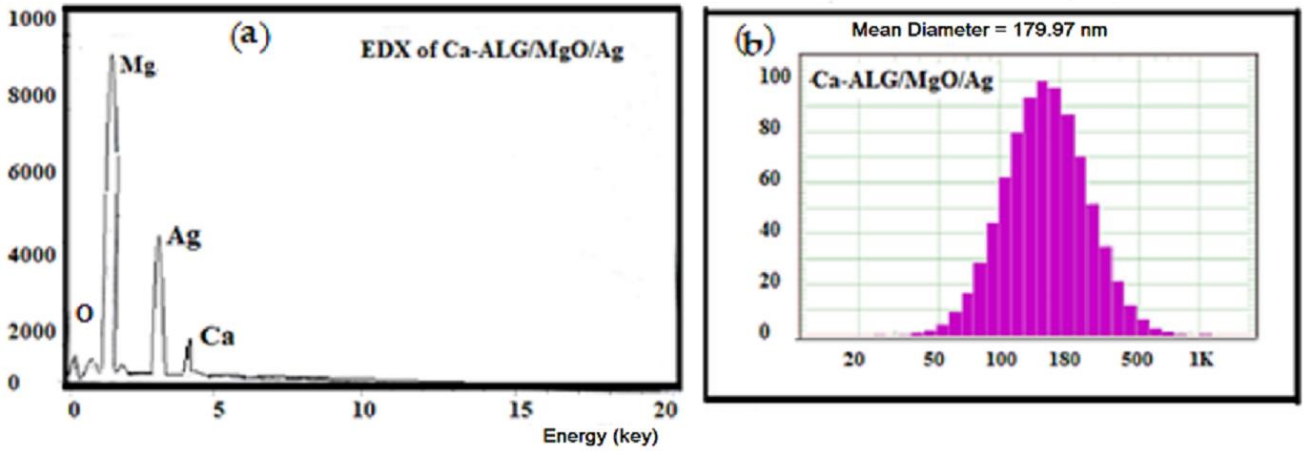

Figure 1. (**a**) EDX and (**b**) DLS diagrams of Ca-ALG/MgO/Ag nanocomposite beads samples.

2.2. TEM and XRD Analysis

Figure 2 illustrates TEM images of Ag NPs and Ca-ALG/MgO/Ag nanocomposite beads, as well as XRD patterns of Ca-ALG/MgO/Ag nanobeads.

The presence of a sharp diffraction peaks combination related to Ag and MgO nanoparticles appeared at 2 Theta = 32°, 45°, and 63°, which are characteristic of MgO nanoparticles [23,24]. For Ag NPs, XRD demonstrated the peaks at 38.17°, 44.28°, 64.5°, 77.52°, and 81.62°, which documented 111, 200, 220, and 311 crystallographic planes of the face-centered cubic silver crystals according to JCPDS (Card No.: 89-3722) [25,26]. The production of Ag NPs doped with MgO NPs within the Ca-ALG beads was confirmed by these findings.

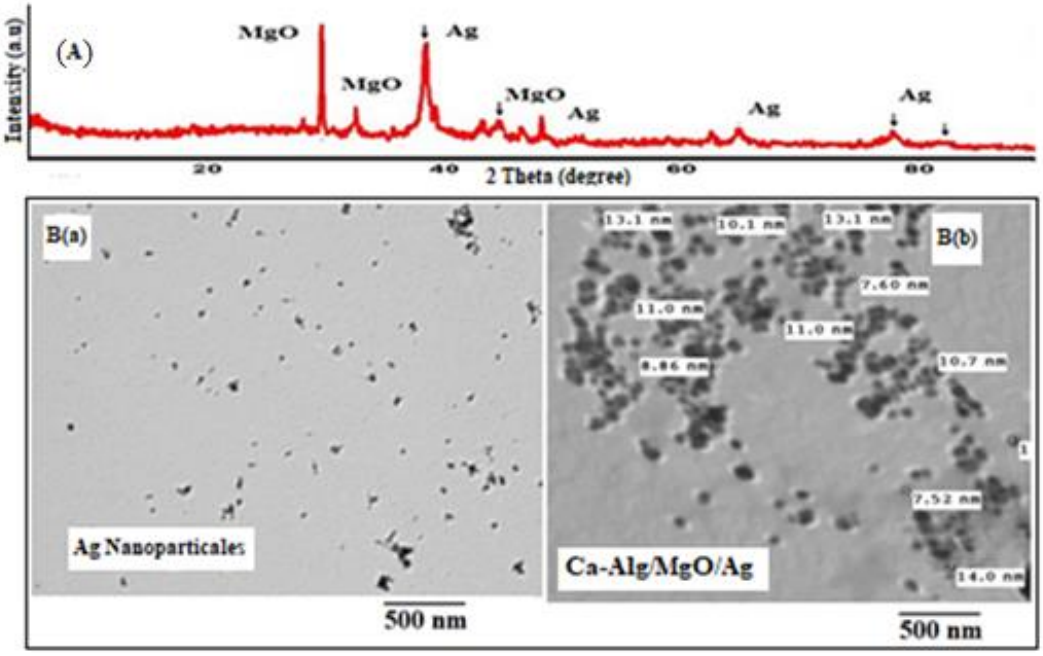

Figure 2. (**A**) XRD pattern of Ca-ALG/MgO/Ag nanocomposite beads, (**B**(**a**)) TEM image of Ag nanoparticles, and (**B**(**b**)) TEM image of Ca-ALG/MgO/Ag nanocomposite beads.

By carrying out the deconvolution of the XRD spectra, it was possible to calculate the particle size (D) of the MgO/Ag NPs using the Debye–Scherrer Equation.

$$D = \frac{K\lambda}{\beta \cos\theta} \quad (1)$$

where D is the particle size, K = 0.89 is the Scherer constant related to crystal shape and index, λ is the X-ray wavelength (1.5406 Å for Cu Kα), θ is the position of the maximum diffraction peak, and β is the line broadening at half the maximum intensity (FWHM in radian). The particles size of MgO/Ag NPs has been found to be around 20 nm.

The TEM is a critical tool for the morphological (size and shape) analysis of nanomaterials. Data from TEM images showed the successful formation of spherical particles of varying sizes that are associated with MgO coupled with Ag NPs with an average particles size of 12 nm for the Ca-ALG/MgO/Ag nanocomposite beads, as shown in Figure 2B(b), while Ag NPs were formed with a size of around 9.5 nm (Figure 2B(a)).

2.3. Catalytic Degradation of Direct Red 83 Dye

The reactive Direct Red 83 dye was used as a model to investigate the catalytic activity of the produced catalyst. The degradation of Direct Red 83 dye using Ca-ALG/MgO/Ag nanocomposite beads at a pH of about 7 has been investigated under different conditions such as $NaBH_4$ content, catalyst amount (0.1–0.5 g), and different initial dye concentrations (10–100 mg/L). The optimization conditions used in the following experiment are 0.3 g of catalyst, 3 mL of $NaBH_4$, starting dye concentration of 100 mg/L, and a total sample volume of 30 mL. Figure 3 shows the UV-Vis spectra for the degradation of Direct Red 83 dye employing Ca-ALG/MgO/Ag nanocomposite beads as a catalyst and $NaBH_4$ as a reducing agent. It was noticed from the degradation, through monitoring the decrease of the absorbance with time, that, at first, the degradation was slow for up to 60 min, and then it started to work properly.

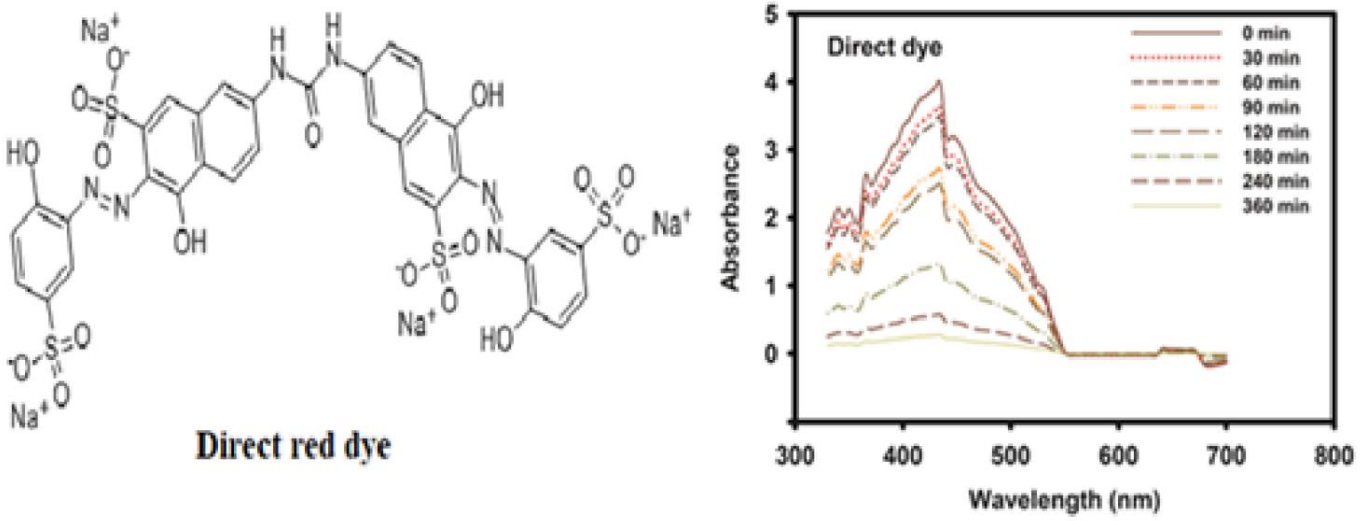

Figure 3. Photo-reduction of Direct Red 83 dye with Ca-ALG/MgO/Ag nanocomposite beads sample under visible light: (catalyst weight 0.3 g, $NaBH_4$ 3 mL, and dye concentration 100 mg/L at λ = 460 nm).

The effect of time on the degradation of Direct Red 83 dye utilizing Ca-ALG/MgO/Ag nanocomposite beads is shown in Figure 4. According to Figure 4, there is a spontaneous decrease in the dye absorbance, which is slow in the first 60 min, and then it increases with time. On the other hand, Figure 4 shows that after 250 min of contact, the degradation percentage of the Direct Red 83 dye utilizing Ca-ALG/MgO/Ag nanocomposite beads as a catalyst reached approximately 95%.

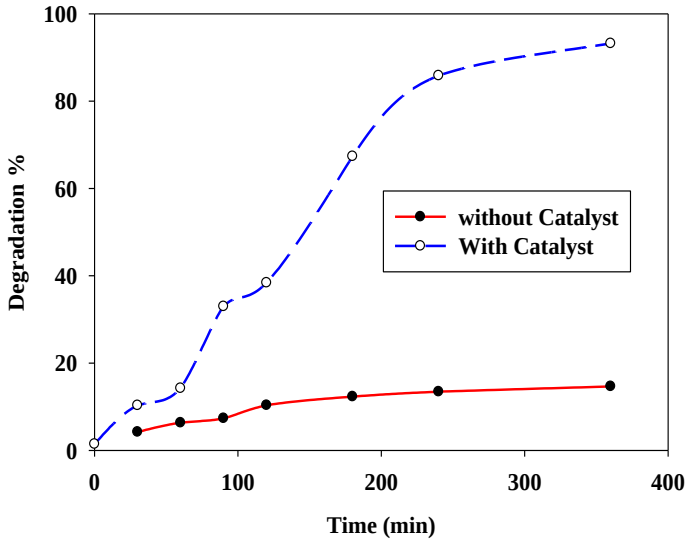

Figure 4. The effect of time on the degradation percentage of Direct Red 83 dye without using a catalyst and with using 0.3 g of catalyst.

2.3.1. Control Experiment

To evaluate the efficiency of the prepared nanocomposite beads catalyst for the degradation of Direct Red 83 dye, the experiment is conducted in the presence and absence of the catalyst. Figure 4 shows the effect of time on the degradation percentage of Direct Red 83 dye with and without using the prepared nanocomposite beads. Figure 4 clearly demonstrates that the degradation percentage of the Direct Red 83 dye without using the prepared Ca-ALG/MgO/Ag nanocomposite beads as a catalyst was very small, nearly 20%, while when the catalyst was added to the degradation reaction, the degradation percentage dramatically increased and reached nearly 95%. These results prove that the catalyst has a great influence on the catalytic degradation of Direct Red 83 dye.

2.3.2. Effect of Catalyst Amount

The standard solution of Direct Red 83 dye 100 mg/L was degraded at 300 min with varied amounts of Ca-ALG/MgO/Ag nanocomposite beads ranging from 0.1 to 0.5 g. The catalyst amount was chosen based on the percentage of dye decolorization that occurred over time. Figure 5 depicts the results of dye degradation at various catalyst amounts. It can be seen that the degradation percentage increases with an increase in the catalyst amount until 0.3 gm. However, beyond 0.3 g, there is no change in the degradation of Direct Red 83 dye. Other researchers also found the same characteristics [27,28]. The result in Figure 5 also reveals that the degradation percentage of the dye increases with an increase in the amount of catalyst Ca-ALG/MgO/Ag nanocomposite beads up to 0.3 g. The increase in the amount of catalyst in the reaction mixture is accompanied by an enhanced generation of $^{\bullet}$OH radicals, which, consequently, increases the rate of degradation. This may be due to the fact that, initially, the increase in the amount of catalyst increases the number of active sites on the catalyst surface, which, in turn, increases the number of hydroxyl radicals. After a certain level of catalyst (0.3 g), the rate of reaction decreases because the dye molecules are not available for adsorption on active sites of the catalyst. The additional catalyst particles, therefore, are not involved in the catalytic activity. Hence the rate of degradation does not increase [29]. Regarding the results obtained, the optimum catalyst amount of 0.3 g at 100 mg/L dye concentration and 3 mL of 1 M $NaBH_4$ showed the highest catalytic degradation of Direct Red 83 dye.

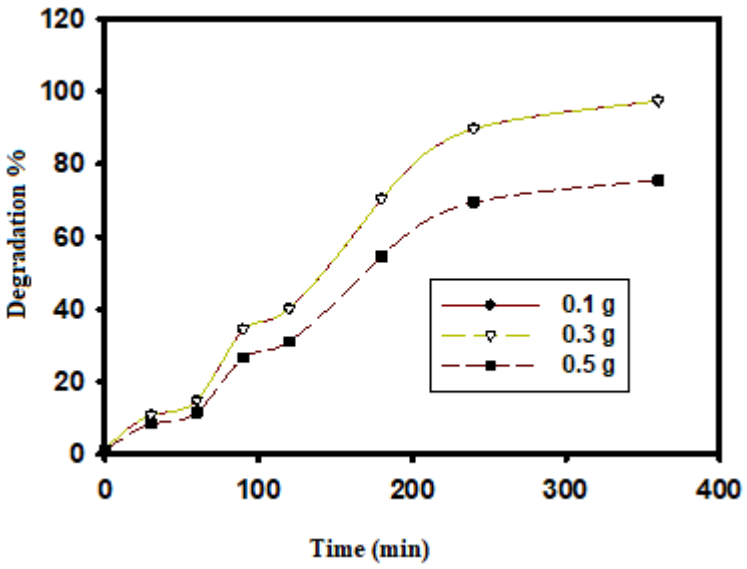

Figure 5. The effect of Ca-ALG/MgO/Ag nanocomposite beads catalyst on the degradation efficiency of Direct Red 83 dye with an initial concentration of 100 mg/L and 3 mL of 1 M $NaBH_4$.

2.3.3. Effect of $NaBH_4$ Content

Figure 6 shows the influence of the reducing agent's content on the catalytic degradation percentage of Direct Red 83 dye using 0.3 g of Ca-ALG/MgO/Ag nanocomposite beads as a catalyst and a Direct Red 83 dye concentration of 100 mg/L as the starting point. As it can be observed, when the amount of 1 M $NaBH_4$ is increased from 3 mL to 5 mL, there is no significant increase in the dye degradation percentage, which leads to the assumption that the amount of reducing agent does not affect the degradation process.

2.3.4. Effect of Initial Direct Red 83 Dye Concentration

The experiments were carried out by varying the concentrations of standard solutions of Direct Red 83 dye from 10 to 100 mg/L with 0.3 g of catalyst and 3 mL of $NaBH_4$. The influence of the initial dye concentration on the catalytic degradation process was observed at 350 min, as shown in Figure 7. The results show that the degradation percentage

decreased with an increase in the initial direct dye concentrations. This can be explained by the fact that the number of •OH radicals formed on the catalyst surface react with dye molecules on the catalyst surface. The increase in the number of dye molecules in solution, with a constant $NaBH_4$ concentration and a constant catalyst amount, leads the catalyst surface to be covered by dye molecules. Therefore, the catalytic efficiency reduces, resulting in a lesser •OH radical generation on the catalyst surface due to the active sites of the catalyst being occupied by the dye molecules [29]. The results indicate insignificant changes in the degradation percentage between 94% and 97% for Ca-ALG/MgO/Ag nanocomposite beads catalyst at higher concentrations from 50 mg/L to 100 mg/L.

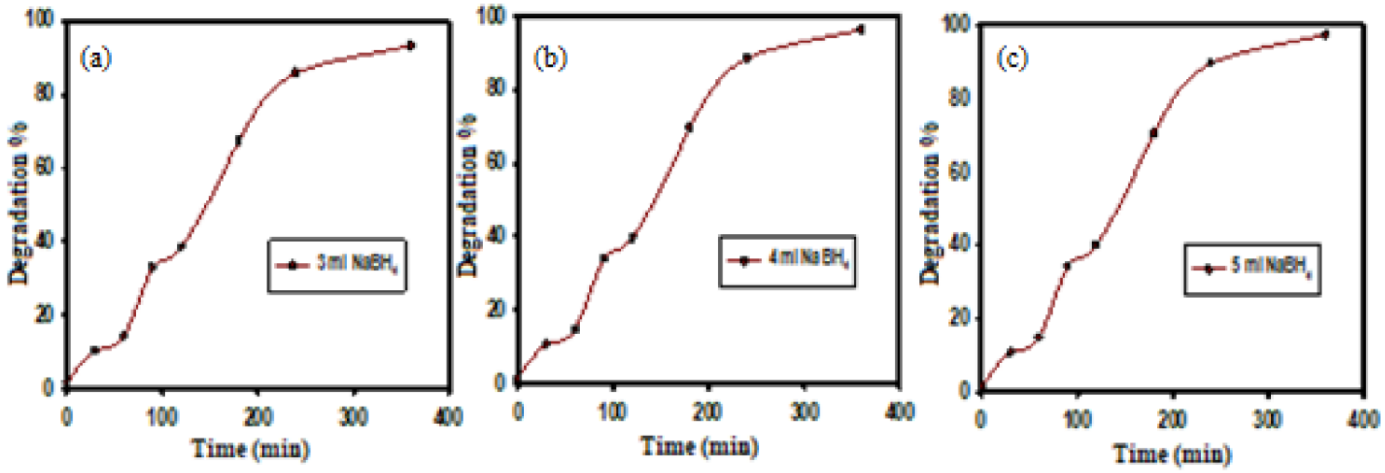

Figure 6. Effect of reducing agent content (**a**) 3 mL, (**b**) 4 mL and (**c**) 5 mL on the degradation of Direct Red 83 dye using 0.3 g of Ca-ALG/MgO/Ag nanocomposite beads catalyst with a dye concentration of 100 mg/L.

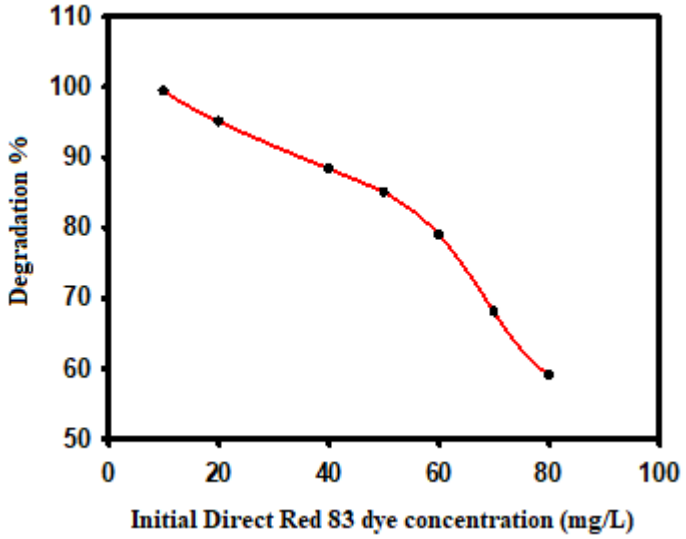

Figure 7. Effect of initial dye concentration (mg/L) on the degradation of Direct Red 83 dye using 0.3 g of Ca-ALG/MgO/Ag nanocomposite beads as a catalyst and 3 mL of $NaBH_4$.

2.3.5. Expected Mechanism for the Degradation of Direct Red 83 Dye

Hassaan et al. [30] reported that direct red 23 dye biologically degraded to oxalic acid and formic acid. Furthermore, Rasool et al. [31] studied direct red 80 dye degradation in the presence of mixed, anaerobic, and sulfate-reducing bacteria culture, wherein the detected metabolites were identified as aniline and 1, 4 diamine benzene that could be further degraded to simpler, final products, H_2O and CO_2. Direct Red 83 dye has a similar structure, so the degradation products could be similar. Figure 8 represents the expected

mechanism for the degradation of Direct Red 83 dye under the effect of the catalytic degradation process using Ca-ALG/MgO/Ag as a catalyst.

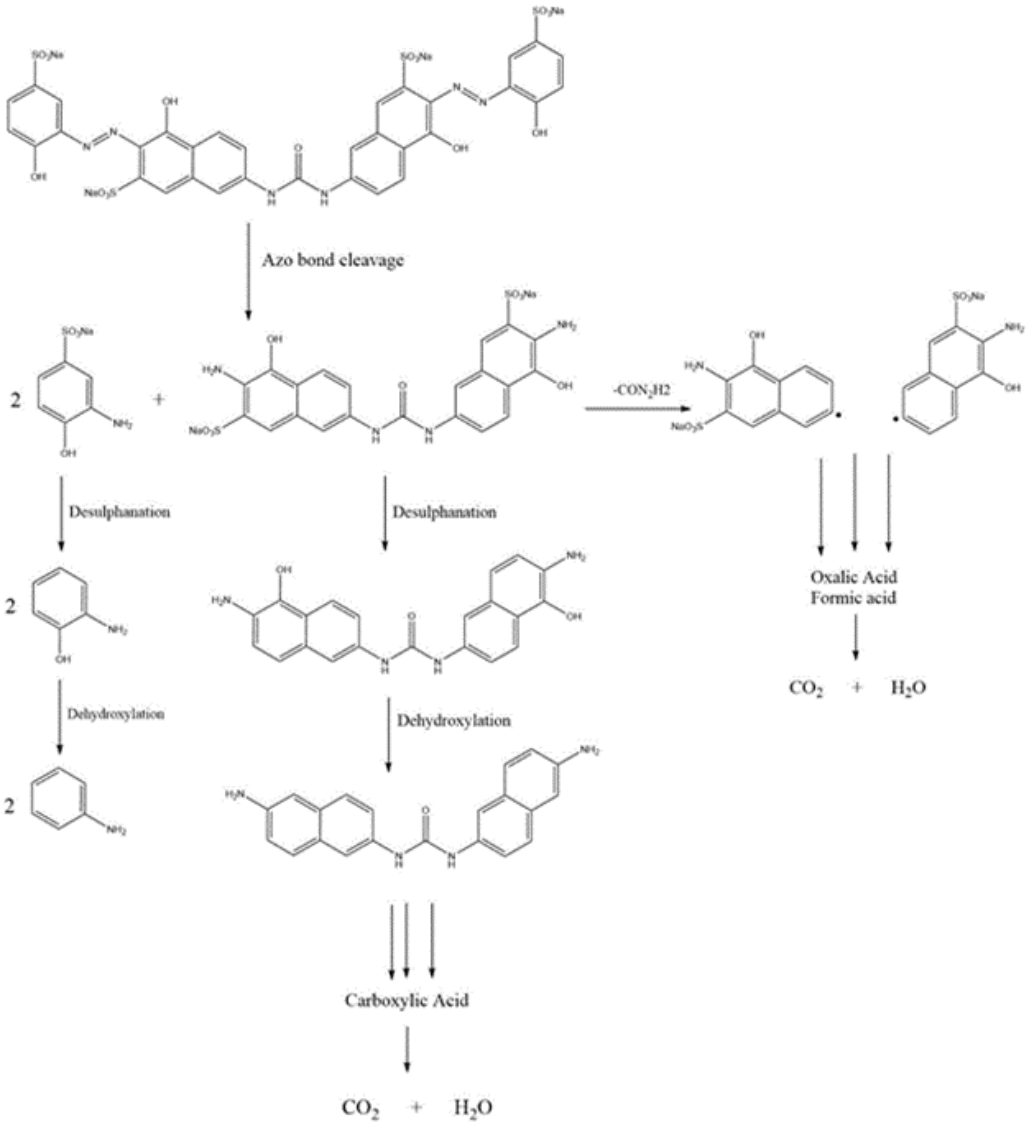

Figure 8. The expected mechanism for the degradation of Direct Red 83 dye.

2.3.6. Adsorption Kinetics

The following kinetic equations [32,33] can be used to estimate the varying rates of dye adsorption. The following equation was used to study pseudo-first-order kinetics for adsorption [34]:

$$Pseudo - first - order\ model : ln(q_e - q_t) = lnq_e - k_1 t \quad (2)$$

The linear form was used for pseudo-second-order kinetics as follows:

$$Pseudo - second - order\ model : \frac{t}{q_t} = \frac{1}{k_2 qe^2} + \frac{t}{q_e} \quad (3)$$

where qt (mg/g) is the adsorption capacity at time t (min), qe (mg/g) is the equilibrium adsorption capacity, and k_1 (min^{-1}) and k_2 (g mg^{-1} min^{-1}) are the rate constants for the pseudo-first-order and pseudo-second-order kinetic models respectively.

2.3.7. Intra-Particle Diffusion Model

The intra-particle diffusion model (IPD) proposed by Weber and Morris has been ap-plied in this study to describe the diffusion mechanism of Direct Red 83 dye molecules into Ca-ALG/MgO/Ag nanocomposite beads as a catalyst [35].

$$q_{t=k_p t^{1/2}+c} \quad (4)$$

The intra-particle rate constant *kp* (mg/g min 1/2) is calculated using a linear plot of qt vs. $t_{1/2}$, where *c* is the intercept. Dye molecules can only diffuse within a particle if the trend lines pass through the origin. Based on the data obtained for the degradation of Direct Red 83 dye using Ca-ALG/MgO/Ag nanocomposite beads as a catalyst and the constraints summarized in Table 1 (Figure 9), pseudo-first-order kinetics is the most appropriate model for the actual degradation processes of direct dye using Ca-ALG/MgO/Ag nanocomposite beads as a catalyst in the presence of $NaBH_4$. The diffusion mechanism during the degradation process passes through multiple stages, which means that intra-particle diffusion is not the main controlling step.

Table 1. Kinetic parameters: pseudo-first-order kinetics, pseudo-second-order kinetics, and intra-particle diffusion model of Direct Red 83 dye degradation.

Polymer Compositions	Pseudo-First-Order		Pseudo-Second-Order		Intra-Particle Diffusion	
	k	R^2	*k*	R^2	k_{id}	R^2
Ca-ALG/MgO/Ag nanocomposite beads	0.95	0.94	0.59	0.787	0.77	0.903

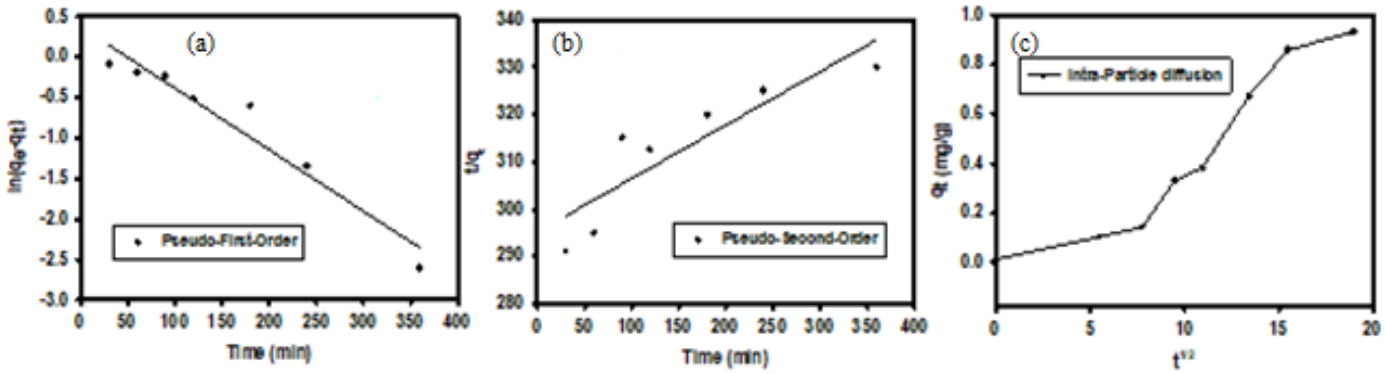

Figure 9. (**a**) pseudo-first-order kinetics, (**b**) pseudo-second-order kinetics, and (**c**) intra-particle diffusion model of Direct Red 83 dye degradation.

2.3.8. Isotherm Analysis

Freundlich, Langmuir, and Temkin isotherms were employed to fit the experimental data in this research.

The Freundlich isotherm model can be used for adsorption on heterogeneous surfaces and multilayer sorption [35]. This model shows that as the sorption centers of an adsorbent are completed, the adsorption energy drops exponentially. The linear form of the Freundlich expression is used to derive this isotherm, which is used to represent heterogeneous catalyst systems:

$$lnq_e = lnK_f + \frac{1}{n} lnC_e \quad (5)$$

where *qe* represents the quantity of dye adsorbed at equilibrium time (mg/g), *Ce* represents the equilibrium concentration of dye in the solution (mg/L), K_f represents the Freundlich constant (L/g) related to the bonding energy, and $1/n$ represents the heterogeneity factor. The slope and intercept of plots *ln qe* versus *ln Ce*, respectively, yield the values of $1/n$ and K_f.

Adsorption occurs on a surface with a finite number of identical sites, according to the Langmuir isotherm model [36]. This is the most well-known adsorption isotherm, commonly used to adsorb pollutants from liquid solutions. The linearized form of the model is given by Equation (6):

$$\frac{C_e}{q_e} = \frac{1}{b\,Q_o} + \frac{1}{Q_o}\,C_e \tag{6}$$

where *Ce* (mg/L) and *qe* (mg/g) are the dye's liquid and solid phase concentrations at equilibrium. Langmuir isotherm constants are K_L (L/g) and a_L (L/mg). The intercept $1/bQ_o$ and slope $(1/Q_o)$ of the linear plot of Ce/qe and *Ce* are used to obtain the constants K_L and a_L. K_L/a_L defines q_{max} as the polymer's maximum adsorption capacity.

The Temkin equation took into account the impact of numerous indirect adsorbate/adsorbent interactions on adsorption isotherms and claimed that the heat of adsorption of all molecules in the layer decreases linearly with coverage as a result of those interactions [37,38]. A consistent distribution of bond energies characterizes adsorption until a bond energy maximum is reached. The Temkin relationship is expressed in the linear form as (7):

$$q_e = \frac{RT}{b_T}\,ln\,a_T + \frac{RT}{b_T}\,ln\,C_e \tag{7}$$

where *T* is the absolute temperature in Kelvin, *R* is the universal gas constant (8.314 J/mol K), a_T is the Temkin isotherm constant (L/g), and b_T is the Temkin constant related to adsorption heat (kJ/mol). The slope and intercept of the linear plot of *qe* vs. *ln Ce* are used to determine the Temkin constants a_T and (RT/b_T)". Figure 10 summarizes the various isothermal relation for the degradation process of Direct Red 83 dye using Ca-ALG/MgO/Ag nanocomposite beads and Table 2 provides the various isothermal models parameters.

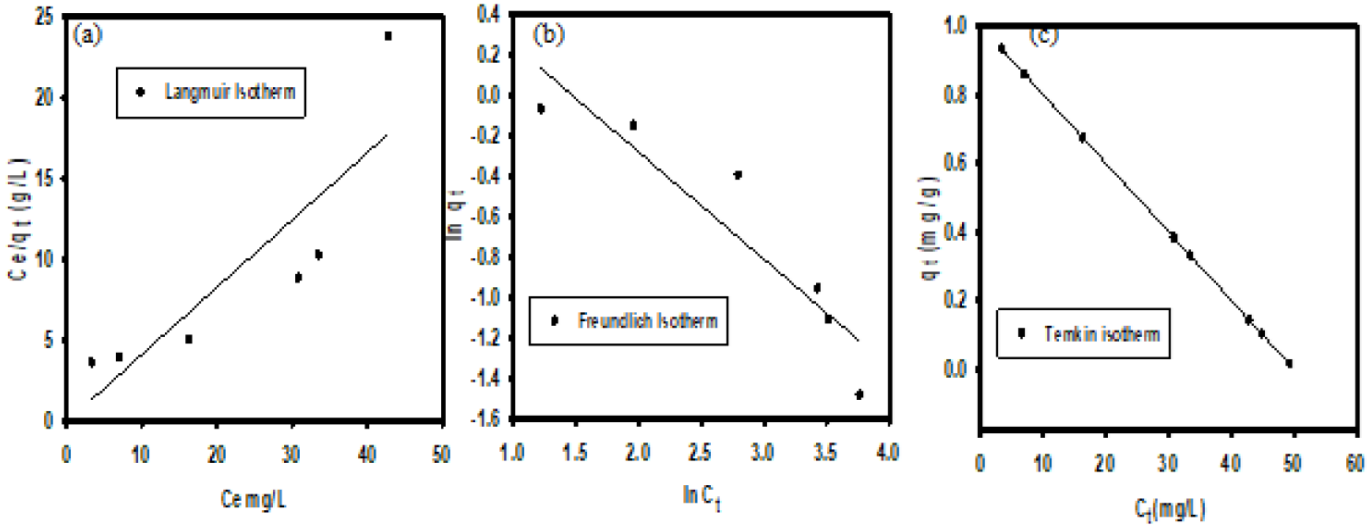

Figure 10. (**a**) Langmuir isotherm model, (**b**) Freundlich isotherm model, and (**c**) Temkin isotherm of Ca-ALG/MgO/Ag nanocomposite beads.

Table 2. Langmuir isotherm model, Freundlich isotherm model, and Temkin isotherm of Ca-ALG/MgO/Ag nanocomposite beads.

Sample	Adsorption Isotherm						
	Langmuir Isotherm Model		Freundlich Isotherm Model			Temkin Isotherm	
	b	R^2	**1/*n***	k_f	R^2	K_t	R^2
Ca-ALG/MgO/Ag	0.75	0.746	0.91	0.91	0.862	0.75	1

Analyzing the data for the isothermal behavior of the degradation of Direct Red 83 dye employing Ca-ALG/MgO/Ag nanocomposite beads as a catalyst gives rise to the conclusion that the best fit for the data is Temkin isotherm, where the R^2 value reached unity, indicating that the reaction is energetically favorable and spontaneous.

3. The Reusability Test of Ca-ALG/MgO/Ag Nanocomposite Beads

The reusability test of the prepared Ca-ALG/MgO/Ag nanocomposite beads as a catalyst for the degradation of Direct Red 83 dye was conducted through continuous four-run recycle under conditions (temperature, 30 °C; reaction time, 48 h; natural pH; catalyst dosage, 0.3 g; initial concentration of dye, 50 mg/L). Figure 11 clearly shows that the degradation percentage of Direct Red 83 dye after four-run recycle decreased to 90% only. The result proved that Ca-ALG/MgO/Ag nanocomposite beads have excellent performance and long-term stability.

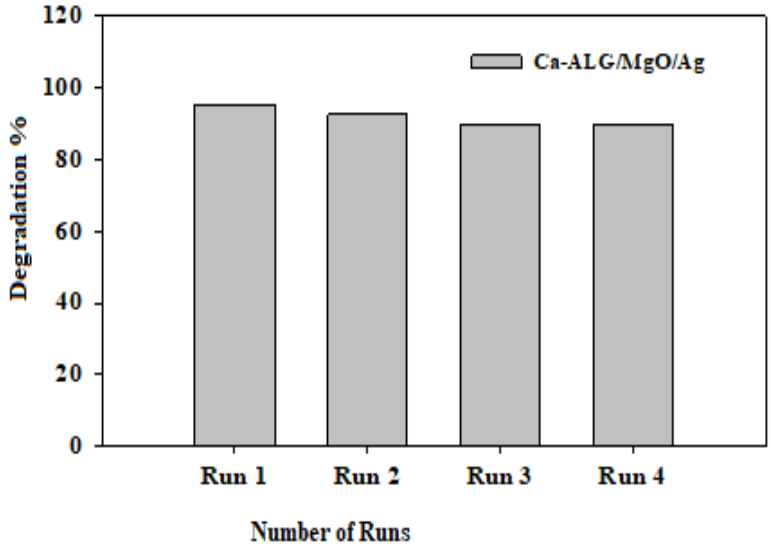

Figure 11. The reusability test of Ca-ALG/MgO/Ag nanocomposites as a catalyst for degradation of Direct Red 83 dye in four consecutive cycles.

4. Materials and Methods

4.1. Materials

Alginic acid sodium salt with medium viscosity (NaAlG) was purchased from Sigma-Aldrich (Gillingham, Dorset, UK); calcium chloride dihydrate ($CaCl_2.2H_2O$) from Algomhoria Co. (Cairo, Egypt); silver nitrate ($AgNO_3$) and magnesium sulfate ($MgSO_4$) from Acros (Thermo Fisher Scientific, Geel, Belgium); and sodium hydroxide (NaOH) (0.5 M) and sodium borohydride (NaBH4) from ADWIC Co. Cairo, Egypt. All materials were purchased at analytical grade and were used as received with double distilled water throughout the study.

4.2. Dye Materials

Sinopharm Chemical Reagent Co. Ltd, Shanghai, China provided the Direct Red 83 dye (analytically pure). The stock solution was made by dissolving a precise amount of dye in deionized water at a concentration of 100 mg/L. Diluting the dye stock solution to a concentration of 20 mg/L yielded the working solutions. The pH variation during the course of the reaction was not significant, so the solutions were prepared at a pH of around 7.

4.3. Preparation of Metal Oxide Nanodispersion

$MgSO_4$ is used as a precursor for the preparation of MgO nanoparticle dispersions by the co-precipitation method using NaOH. A solution of 1% *wt*/*v* of $MgSO_4$ was prepared, and 150 mL of it was vigorously stirred on a magnetic stirrer, following which 200 mL of 1 M

NaOH was added, drop by drop, very slowly, until a milky-white suspension was formed. The formed dispersion was left to settle down, and the excess volume of supernatant was decanted very slowly. The milky-white suspension was washed and distilled by adding an excess of distilled water, following which it was decanted several times to remove excess NaOH, and, subsequently, the MgO dispersion volume was completed to 100 mL with distilled water. After this, the prepared nanoparticle dispersions were placed in a carefully sealed bottle for further use and characterization.

4.4. Preparation of Ca-ALG/MgO Nanobeads

The amount of 10% *wt*/*v* of MgO nanodispersion was added in beakers containing a suitable volume of alginate solution at a concentration of 3% *wt*/*v* prepared by dissolving 3 g in 100 mL of distilled water, and magnetic stirring was used to thoroughly combine the ingredients until they became completely homogenous. The ALG/MgO (90/10) (*v*/*v*) mixtures were dropped carefully into a solution of $CaCl_2.2H_2O$ (concentrations 3% *wt*/*v*) under magnetic stirring using a 5 mL syringe. Nanobeads formed instantly, and finally, they were rinsed gently with distilled water and dried at room temperature.

4.5. Preparation of Silver Containing Ca-Alginate/MgO Nanocomposite Beads

The nanobeads from the previous stage were soaked overnight in a beaker containing 50 mL of $AgNO_3$ solution (1 M). The beaker was covered with an aluminum foil and left overnight to entrap Ag+ ions. After that, the beads were removed, washed carefully, and then transferred to a beaker containing 50 mL of 0.5 M $NaBH_4$ as a reducing agent for 2 h to reduce the entrapped Ag^+ ions to Ag NPs. The beads instantly turned black, which indicated the formation of Ag NPs. Subsequently, the Ca-Alginate/MgO/Ag nanocomposite beads were removed, washed, and dried. Figure 12 illustrates the preparation steps of Ca-Alginate/MgO/Ag nanocomposite beads supported with digital photos.

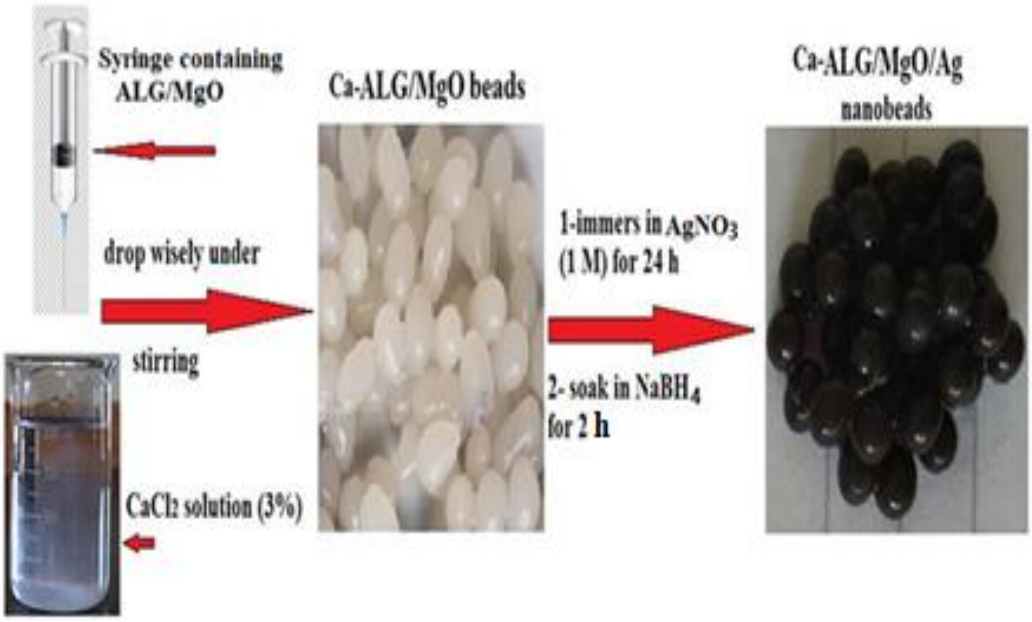

Figure 12. Steps of preparation of Ca-ALG/MgO/Ag nanocomposite beads supported with digital photos.

4.6. The Catalytic Degradation of Direct Red 83 Dye

The degradation of Direct Red 83 dye was carried out at 30 °C. In this experiment, 30 mL of aqueous Direct Red 83 dye solution (100 mg/L) was added to a beaker containing 0.3 g of Ca-ALG/MgO/Ag nanocomposite beads (used as a catalyst) and stirred for 30 min, after which 3 mL of 1 M $NaBH_4$ was added, and the dye solution's absorbance was measured using a UV-Vis spectroscope over the 300 nm wavelength. The reaction mixture

was then continuously stirred with a magnetic stirrer for the whole reaction time. The extent of dye degradation was calculated using the relation:

$$Degradation\% = \frac{A_o - A_t}{A_o} \times 100 \quad (8)$$

where A_o is the initial absorbance of the dye solution and A_t is the absorbance at different time intervals.

4.7. Effect of Different Parameters on Catalytic Degradation of Direct Red 83 Dye

4.7.1. Effect of Catalyst Amount

The standard solution of Direct Red 83 dye (100 mg/L) was degraded at 300 min with varied amounts of Ca-ALG/MgO/Ag nanocomposite beads (0.1, 0.3, 0.5 g) at 30 °C, 3 mL of $NaBH_4$.

4.7.2. Effect of $NaBH_4$ Content

The influence of the reducing agent's content on the catalytic degradation percent was studied from 3 to 5 mL at 30 °C using 0.3 g of Ca-ALG/MgO/Ag nanocomposite beads as a catalyst and a Direct Red 83 dye concentration of 100 mg/L.

4.7.3. Effect of Initial Direct Red 83 Dye Concentration

The experiments were carried out by varying the concentrations of standard solutions of Direct Red 83 dye from 10 to 100 mg/L with 0.3 g of catalyst and 3 mL of $NaBH_4$.

4.8. Kinetic Studies

Adsorption kinetic experiments were carried out using a shaker water bath. The entire dye solution was prepared with distilled water. Kinetic experiments were carried out by agitating a 50 mL solution of a constant dye concentration (100 mg/L with 0.3 g of Ca-ALG/MgO/Ag nanocomposite beads at a constant agitation speed, 30 °C, and pH of around 7. Agitation was made for 340 min at a constant stirring speed of 120 rpm. Next, 2 mL samples were drawn at suitable time intervals. The samples were then centrifuged for 15 min at 5000 rpm, and the left-out concentration in the supernatant solution was analyzed using UV–Vis spectrophotometer (Starna Scientific Ltd., Hainault, Essex, UK) by monitoring the absorbance changes at a wavelength of maximum absorbance. Each experiment continued until equilibrium conditions were reached at 340 min when no further decrease in the dye concentration was measured. Calibration curves were plotted between absorbance and concentration of the dye solution.

4.9. Characterizations

Using a Bruker Vertex 70 FTIR spectrometer made in Bremen, Germany, IR spectroscopy was applied between 4000–400 cm^{-1} at a tenacity of 4 cm^{-1}. XRD investigations were carried out on an Ultima IV (Rigaku International Corp., Tokyo, Japan) with Cu-Kα radiation of λ = 1.54 Å in the 2θ range from 5° to 80°. TEM was performed for the determination of the particle size in the nanocomposite beads on a JEOL JEM-100CX made in Tokyo, Japan. The particle distribution of Ca-ALG/MgO/Ag nanocomposite was estimated by DLS (DLS-ZP/Particle Sizer Nicomp 380ZLS, made in Chandler, AZ, USA). EDX analysis of Ca-ALG/MgO/Ag nanocomposite was performed using a field emission scanning electron microscope (FEI Nova NanoSEM 650) made in Riga, Latvia.

5. Conclusions

The catalytic performance of Ca-ALG/MgO/Ag nanocomposite beads for the reduction of Direct Red 83 dye was investigated using $NaBH_4$ as a reducing agent. Different amounts of the prepared catalyst in the range of 0.1–0.5 were employed to study the effect of the catalyst amount on the degradation rate. The control experiment proved that the maximum rate of degradation was observed when the amount of catalyst was 0.3 g, and that this amount was

sufficient to degrade 50 mL of dye solution at a concentration of 100 mg/L. Additionally, the relation between the degradation rate and $NaBH_4$ concentration was investigated. The results showed that there was no significant increase in the dye degradation percentage, assuming that the amount of reducing agent does not affect the degradation process. After 300 min of adding $NaBH_4$ to an aqueous solution of Direct Red 83 dye in the presence of catalytic beads, the color of the solution changed from red to colorless. The adsorption isotherms were evaluated using the Langmuir, Freundlich, and Temkin isotherm models. The adsorption process was best described by the Temkin isotherm with R^2 of 1. Furthermore, kinetics study revealed that the degradation process using Ca-ALG/MgO/Ag nanocomposite beads was the best fit for the pseudo-first-order model. Moreover, Ca-ALG/MgO/Ag was found to exhibit excellent long-term stability. This excellent catalytic activity and stability suggest that Ca-ALG/MgO/Ag nanocomposite beads can be a potential candidate for the treatment of industrially discharged wastewater.

Funding: This research was founded by [The Deanship of Scientific Research at Prince Sattam bin Abdulaziz University] grant number [# 2017/01/6933].

Data Availability Statement: The raw data applied to discuss these results cannot be shared at this time.

Acknowledgments: The project was supported by the deanship of scientific research at Prince Sattam bin Abdulaziz University under research project # 2017/01/6933.

Conflicts of Interest: The authors declare that they have no conflict of interest.

References

1. Semeraro, P.; Fini, P.; D'Addabbo, M.; Rizzi, V.; Cosma, P. Removal from wastewater and recycling of azo textile dyes by alginate-chitosan beads. *Int. J. Agric. Environ. Biotechnol.* **2017**, *2*, 1835–1850. [CrossRef]
2. Benkaddour, S.; Slimani, R.; Hiyane, H.; El Ouahab, I.; Hachoumi, I.; El Antri, S.; Lazar, S. Removal of reactive yellow 145 by adsorption onto treated watermelon seeds: Kinetic and isotherm studies, Sustain. *Chem. Pharm.* **2018**, *10*, 16–21. [CrossRef]
3. Slama, H.; Bouket, A.C.; Pourhassan, Z.; Alenezi, F.N.; Silini, A.; Cherif-Silini, H.; Oszako, T.; Luptakova, L.; Golinska, P.; Belbahr, L. Diversity of Synthetic Dyes from Textile Industries, Discharge Impacts and Treatment Methods. *Appl. Sci.* **2021**, *11*, 6255. [CrossRef]
4. Bettin, F.; Cousseau, F.; Martins, K.; Zaccaria, S.; Girardi, V.; Silveira, M.M.; Dillon, A.J.P. Effects of pH, Temperature and Agitation on the Decolourisation of Dyes by Laccase-Containing Enzyme Preparation from Pleurotus sajor-caju. *Braz. Arch. Biol. Technol.* **2019**, *62*, e19180338:1–19180338:22. [CrossRef]
5. Shahzad, K.; Hussain, S.; Altaf Nazir, M.; Jamshaid, M.; Rehman, A.; Alkorbi, A.S.; Alsaiari, R.; Alhemiary, N.A. Versatile Ag_2O and ZnO nanomaterials fabricated via annealed Ag-PMOS and ZnO-PMOS: An efficient photocatalysis tool for azo dyes. *J. Mol. Liq.* **2022**, *356*, 119036. [CrossRef]
6. Shahzad, K.; Imran Khan, M.; Shanableh, A.; Elboughdiri, N.; Jabeen, S.; Altaf Nazir, M.; Farooq, N.; Ali, H.; Abdelfattah, A.; Rehman, A. Silver supported-Ag@PMOS onto thumb structured porous organosilica materials with efficient hetero-junction active sites for photodegradation of methyl orange dye. *Inorg. Nano-Met. Chem.* **2022**, *52*, 407–416. [CrossRef]
7. Thakur, V.; Kumar, P.; Verma, A.; Chand, D. Decolorization of dye by alginate immobilized laccase from Cercospora SPF-6: Using compact 5 stage plug flow reactor. *Int. J. Curr. Microbiol. Appl. Sci.* **2015**, *4*, 183–200.
8. Shaban, M.; Abukhadra, M.R.; Ibrahim, S.S.; Shahien, M.G. Photocatalytic degradation and photo-Fenton oxidation of Congo red dye pollutants in water using natural chromite—Response surface optimization. *Appl. Water Sci.* **2017**, *7*, 4743–4756. [CrossRef]
9. Jamshaid, M.; Altaf Nazir, M.; Najam, T.; Ahmad Shah, S.S.; Khan, H.M.; Rehman, A. Facile synthesis of Yb^{3+}-Zn^{2+} substituted M type hexaferrites: Structural, electric and photocatalytic properties under visible light for methylene blue removal. *Chem. Phys. Lett.* **2022**, *805*, 139939. [CrossRef]
10. Alotaibi, K.M.; Almethen, A.A.; Beagan, A.M.; Al-Swaidan, H.M.; Ahmad, A.; Bhawani, S.A.; Alswieleh, A.M. Quaternization of Poly(2-diethyl aminoethyl methacrylate) Brush-Grafted Magnetic Mesoporous Nanoparticles Using 2-Iodoethanol for Removing Anionic Dyes. *Appl. Sci.* **2021**, *11*, 10451. [CrossRef]
11. Karthiga Devi, G.; Senthil Kumar, P.; Sathish Kumar, K. Green synthesis of novel silver nanocomposite hydrogel based on sodium alginate as an efficient biosorbent for the dye wastewater treatment: Prediction of isotherm and kinetic parameters. *Desalin Water Treat.* **2016**, *57*, 27686–27699. [CrossRef]
12. Singh, R.; Singh, D. Radiation synthesis of PVP/alginate hydrogel containing nanosilver as wound dressing. *J. Mater. Sci. Mater. Med.* **2012**, *23*, 2649–2658. [CrossRef]
13. Da Silva Fernandes, R.; de Moura, M.R.; Glenn, G.M.; Aouada, F.A. Thermal, microstructural, and spectroscopic analysis of Ca2+ alginate/clay nanocomposite hydrogel beads. *J. Mol. Liq.* **2018**, *265*, 327–336. [CrossRef]

14. Harikumar, P.S.; Aravind, A. Antibacterial Activity of Copper Nanoparticles and Copper Nanocomposites against Escherichia Coli Bacteria. *Int. J. Sci.* **2016**, *5*, 83–90. [CrossRef]
15. Fadillah, G.; Serunting, M.A. Preliminary Study of Photocatalytic Degradation of Methylene Blue Dye using Magnetic Alginate/Fe3O4 (Alg/Fe3O4) Nanocomposites. *EKSAKTA J. Sci. Data Anal.* **2019**, *19*, 26–34. [CrossRef]
16. Wang, X.Q.; Han, S.F.; Zhang, Q.W.; Zhang, N.; Zhao, D.D. Photocatalytic oxidation degradation mechanism study of methylene blue dye waste water with GR/iTO$_2$. *MATEC Web Conf.* **2018**, *238*, 03006:1–03006:5. [CrossRef]
17. Ajmal, A.; Majeed, I.; Malik, R.N.; Idriss, H.; Nadeem, M.A. Principles and mechanisms of photocatalytic dye degradation on TiO_2 based photocatalysts: A comparative overview. *RSC Adv.* **2014**, *4*, 37003–37026. [CrossRef]
18. Chiu, Y.H.; Chang, T.M.; Chen, C.Y.; Sone, M.; Hsu, Y.J. Mechanistic Insights into Photodegradation of Organic Dyes Using Heterostructure Photocatalysts. *Catalysts* **2019**, *9*, 430:1–430:32. [CrossRef]
19. Albalwi, H.; Abou El Fadl, F.I.; Ibrahim, M.M.; Abou Taleb, M.F. Catalytic activity of silver nanocomposite alginate beads for degradation of basic dye: Kinetic and isothermal study. *Appl. Organomet. Chem.* **2021**, *36*, e6490. [CrossRef]
20. Alimard, P. Fabrication and kinetic study of Nd-Ce doped Fe_3O_4-chitosan nanocomposite as catalyst in Fenton dye degradation. *Polyhedron* **2019**, *171*, 98–107. [CrossRef]
21. Amorim, N.; Nascimento, G.; Charamba, L.; Rocha Santana, R.; Da Silva, P.; Napoleão, T.; Napoleão, D. Direct red 83 textile dye degradation using photoperoxidation and photo-fenton: Kinetic studies, toxicity and neural networks modeling. *Ciência Nat.* **2020**, *42*, e41. [CrossRef]
22. León, G.; Miguel, B.; Manzanares, L.; Saavedra, M.I.; Guzmán, M.A. Kinetic Study of the Ultrasound Effect on Acid Brown 83 Dye Degradation by Hydrogen Peroxide Oxidation Processes. *Chem. Eng. J.* **2021**, *5*, 52. [CrossRef]
23. El-Sawy, N.M.; Raafat, A.I.; Badawy, N.A.; Mohamed, A.M. Radiation development of pH-responsive (xanthan-acrylic acid)/MgO nanocomposite hydrogels for controlled delivery of methotrexate anticancer drug. *Int. J. Biol. Macromol.* **2020**, *142*, 254–264. [CrossRef] [PubMed]
24. Abdel Ghaffar, A.M.; Abou El Fadl, F.I.; El-Sawy, N.M. Radiation synthesis of polyvinyl alcohol/acrylic acid/magnesium oxide composite hydrogel for removal of boron from its aqueous solution. *J. Thermoplast. Compos. Mater.* **2020**, *35*, 1022–1040. [CrossRef]
25. Iqbal, M.; Naseem, T.; Waseem, M.; Din, S.U.; Hafeez, M.; Haq, S.; Qureshi, S.; Bibi, A.; Rehman, S.U.; Hussain, R.; et al. Synthesis and Characterization of rGO/Ag_2O Nanocomposite and its Use for Catalytic Reduction of 4-Nitrophenol and Photocatalytic Activity. *J. Inorg. Organomet. Polym. Mater.* **2021**, *31*, 100–111. [CrossRef]
26. Mandava, K. Biological and non-biological synthesis of metallic nanoparticles: Scope for current pharmaceutical research. *Indian J. Pharm. Sci.* **2017**, *79*, 501–512. [CrossRef]
27. Zangeneh, H.; Zinatizadeh, A.A.L.; Habibi, M.; Akia, M.; Isa, M.H. Photocatalytic oxidation of organic dyes and pollutants in wastewater using different modified titanium dioxides: A comparative review. *J. Ind. Eng. Chem.* **2015**, *26*, 1–36. [CrossRef]
28. Sahoo, P.K.; Thakur, D.; Bahadur, D.; Panigrahy, B. Highly efficient and simultaneous catalytic reduction of multiple dyes using recyclable RGO/Co dendritic nanocomposites as catalyst for wastewater treatment. *RSC Adv.* **2016**, *6*, 106723–106731. [CrossRef]
29. Reza, K.M.; Kurny, A.S.W.; Gulshan, F. Parameters affecting the photocatalytic degradation of dyes using TiO_2: A review. *Appl. Water Sci.* **2017**, *7*, 1569–1578. [CrossRef]
30. Hassaan, M.A.; El Nemr, A.; El-Zahhar, A.A.; Idris, A.M.; Alghamdi, M.M.; Sahlabji, T.; Said, T.O. Degradation mechanism of Direct Red 23 dye by advanced oxidation processes: A comparative study. *Toxin Rev.* **2020**, *41*, 38–47. [CrossRef]
31. Rasool, K.; Woo, S.H.; Lee, D.S. Simultaneous removal of COD and Direct Red 80 in a mixed anaerobic sulfate-reducing bacteria culture. *Chem. Eng. J.* **2013**, *223*, 611–616. [CrossRef]
32. Tang, Y.; Yang, R.; Ma, D.; Zhou, B.; Zhu, L.; Yang, J. Removal of methyl orange from aqueous solution by adsorption onto a hydrogel composite. *Polym. Polym. Compos.* **2018**, *26*, 161–168. [CrossRef]
33. Singh, T.; Singhal, R. Kinetics and thermodynamics of cationic dye adsorption onto dry and swollen hydrogels poly(acrylic acid-sodium acrylate-acrylamide) sodium humate. *Desalin Water Treat.* **2013**, *53*, 3668–3680. [CrossRef]
34. Boulaiche, W.; Hamdi, B.; Trari, M. Removal of heavy metals by chitin: Equilibrium, kinetic and thermodynamic studies. *Appl. Water Sci.* **2019**, *9*, 10. [CrossRef]
35. Miyah, Y.; Lahrichi, A.; Idrissi, M.; Boujraf, S.; Taouda, H.; Zerrouq, F. Assessment of adsorption kinetics for removal potential of Crystal Violet dye from aqueous solutions using Moroccan pyrophyllite. *J. Assoc. Arab Univ. Basic Appl. Sci.* **2017**, *23*, 20–28. [CrossRef]
36. Awad, F.S.; Abou Zied, K.M.; Abou El-Maaty, W.M.; El-Wakil, A.M.; El-Shall, M.S. Effective removal of mercury(II) from aqueous solutions by chemically modified graphene oxide nanosheets. *Arab. J. Chem.* **2020**, *13*, 2659–2670. [CrossRef]
37. Xie, S.; Wen, Z.; Zhan, H.; Jin, M. An Experimental Study on the Adsorption and Desorption of Cu(II) in Silty Clay. *Geofluids* **2018**, *2018*, 3610921. [CrossRef]
38. Priyadarshini, B.; Rath, P.P.; Behera, S.S.; Panda, S.R.; Sahoo, T.R.; Parhi, P.K. Kinetics, Thermodynamics and Isotherm studies on Adsorption of Eriochrome Black-T from aqueous solution using Rutile TiO_2. *IOP Conf. Ser. Mater. Sci. Eng.* **2018**, *310*, 012051:1–012051:13. [CrossRef]